Journal of Architectural Research and Development, 2026, Volume 10, Issue 5
https://bbwpublisher.com/journal/JARD
Online ISSN: 2208-3537
Print ISSN: 2208-3529

Study on Seepage and Deformation Responses during Tunnel Excavation and the Influence of Support Parameters

Xizhen Wang

School of Civil Engineering, Shijiazhuang Tiedao University, Shijiazhuang 050043, Hebei, China

Copyright: © 2026 Author(s). This is an open-access article distributed under the terms of the Creative Commons Attribution License (CC BY 4.0), permitting distribution and reproduction in any medium, provided the original work is cited.

Abstract: To investigate the evolution characteristics of groundwater seepage and surrounding rock deformation during tunnel excavation and the effectiveness of support control, a steady-state seepage model and an elastoplastic mechanical model were developed for a deep-buried circular tunnel. The spatial distributions of the seepage and displacement fields and their responses to construction steps under the bench excavation method were analyzed, and the effects of the thickness, elastic modulus, and permeability coefficient of the primary support and grouting ring were examined. The results indicate that after excavation, groundwater converges toward the tunnel cavity and tunnel face, while the surrounding rock deforms toward the excavated space; the more significant responses are mainly concentrated around the tunnel periphery and near the tunnel face. As the excavation face approaches and passes the studied section, the peripheral displacement and outflow change rapidly and then gradually stabilize. Increasing the thickness of the primary support and grouting ring reduces the peripheral displacement and water inflow, but the incremental control effect diminishes with increasing thickness. Increasing the elastic modulus of the primary support and grouting reinforcement zone is beneficial for controlling surrounding rock deformation, whereas reducing their permeability coefficients can effectively decrease tunnel water inflow. When the water-blocking capacity of the primary support is enhanced, the external water pressure on the lining increases; when the water-blocking capacity of the grouting ring is enhanced, the external water pressure on the lining decreases. These results can provide a reference for selecting support and grouting parameters for tunnels in water-rich surrounding rock.

Keywords: Tunnel engineering; Steady-state seepage; Surrounding rock deformation; Primary support; Grouting reinforcement

Online publication: Oct 13, 2026

1. Introduction

Excavation of a tunnel in water-rich surrounding rock simultaneously alters the stress state of the ground and the groundwater drainage conditions. After the surrounding rock is unloaded, stress redistribution and

deformation occur around the tunnel periphery, while groundwater converges toward the newly formed drainage boundary. Water inflow not only increases the burden of construction drainage but may also affect the stability of the surrounding rock and the forces acting on the support structures. Therefore, understanding the spatial distribution and evolution characteristics of seepage and deformation during excavation, and clarifying the control effects of support and grouting measures, constitute an important basis for selecting tunnel construction parameters.

With respect to the mechanical and permeability characteristics of rock masses under unloading conditions, previous studies have conducted triaxial tests on limestone, dolomite, and sandstone, revealing the relationships between fracture opening, damage development, and permeability variation [1–3]. Unloading tests on sandstone and marble indicate that the unloading path and initial stress conditions affect rock deformation and mechanical parameters; seepage studies on fractured rock masses have further analyzed the evolution characteristics of flow channels during unloading [4–7]. At the tunnel scale, the surrounding rock conditions, support performance, and groundwater boundary jointly govern the response around the tunnel, and primary support and grouting reinforcement are important measures for controlling deformation and water inflow [8–10].

Primary support shares the surrounding rock load by constraining peripheral deformation, whereas grouting provides reinforcement and water-blocking effects by improving the mechanical properties and reducing the permeability of the surrounding rock. The thickness and material properties of these two measures directly affect their control effectiveness, and their effects also vary with the advancement of the tunnel face and the installation of support. An integrated analysis of the construction process and support parameters is helpful for identifying the key response locations, control timing, and parameter variation patterns.

This study focuses on a deep-buried circular tunnel and establishes a staged steady-state seepage model and an elastoplastic mechanical model. First, the spatial distributions of seepage and displacement induced by bench excavation are analyzed. Subsequently, the variations in the response of a typical section with construction steps are compared. Finally, the effects of the thickness, stiffness, and permeability of the primary support and grouting ring are investigated, and the control patterns of these two measures on surrounding rock deformation, water inflow, and external water pressure on the lining are summarized.

2. Numerical model and calculation cases

2.1. Model and construction process

The tunnel has an excavation radius of 8 m and a burial depth of 300 m. It is constructed using the bench excavation method, with a round length of 2 m per cycle and a bench spacing of 4 m between the upper and lower benches. In the construction process analysis, the primary support consists of 0.25 m thick C25 shotcrete and lags the excavation by one cycle. The crown, haunch, and invert are selected as monitoring locations. The response to construction steps is analyzed at a section 10 m from the tunnel portal, while the influence of support parameters is analyzed at a section in the middle of the tunnel.

Mechanical analysis was performed using FLAC3D. The model dimensions in the transverse, vertical, and longitudinal directions were 200, 200, and 50 m, respectively. The surrounding rock and grouting reinforcement zone were modeled using the Mohr–Coulomb constitutive model, while the support and lining were simulated using solid elements. The bottom boundary of the model was constrained in all three

displacement directions, and the four lateral boundaries were constrained in the normal direction. For the construction process case, the lateral pressure coefficient was 1.2, and an equivalent load of 4.6 MPa was applied at the top; for the support parameter case, the lateral pressure coefficient was 1.1, and the equivalent top load was 4.0 MPa. These equivalent top loads correspond to the self-weight of the 200 m overlying strata above the model.

Seepage analysis was performed using MIDAS. The construction process model has dimensions of 1600 m × 600 m × 50 m, while a longitudinal thickness of 1 m is adopted for the support parameter analysis. The bottom boundary of the model is impermeable, the left and right lateral boundaries are prescribed with a total head of 300 m, the exposed excavation surfaces are set as zero-pressure-head boundaries, and the support and lining are assigned finite permeability coefficients. As the bench advances, the excavation and support domains are updated sequentially, and the steady-state seepage field is solved for each construction stage.

2.2. Material parameters and variable settings

The surrounding rock and support parameters were selected according to relevant specifications and the literature, and the main values are listed in **Table 1** [8–10]. The construction process analysis and the support parameter analysis adopted their respective baseline cases, and within each parameter group, the model boundaries, construction method, and other material parameters were kept consistent. In the support parameter analysis, the secondary lining is 0.30 m thick and lags 10 m behind the primary support in the mechanical construction simulation.

Table 1. Material parameters of surrounding rock and support

Working conditions and materials	E/GPa	c/MPa	φ/(°)	γ/(kN/m³)	ν	k/(m/s)
Construction process surrounding rock	1.3	0.25	22	23	0.35	1×10^{-5}
Construction process primary support	28	1.5	50	24	0.18	9.26×10^{-10}
Parameter analysis surrounding rock	1.3	0.25	27	20	0.24	1×10^{-6}
Parameter analysis primary support	28	—	—	24	0.18	1×10^{-8}
Parameter analysis secondary lining	30	—	—	25	0.20	1×10^{-10}
Parameter analysis grouting ring	6.4	0.85	45	26	0.25	1×10^{-7}

Note: E, elastic modulus; c, cohesion; φ, internal friction angle; γ, unit weight; ν, Poisson's ratio; k, permeability coefficient.

In the thickness analysis, the primary support thicknesses were set to 0.10, 0.15, 0.20, 0.30, and 0.50 m, and the grouting ring thicknesses were set to 1, 3, 5, 7, and 9 m. In the stiffness analysis, the elastic modulus of the primary support was set to 15, 20, 24, 28, 35, 50, 60, and 70 GPa, and that of the grouting reinforcement zone was set to 1, 2, 3, 5, 7, and 10 GPa.

In the permeability analysis, the permeability coefficient ratio of adjacent materials was adopted as the variable. In the primary support analysis, the permeability coefficient of the grouting ring was fixed at $k_g = 1 \times 10^{-7}$ m/s, and the primary support permeability coefficient kl was varied such that kg/kl was set to 2, 4, 8, 12, 20, 100, and 200. In the grouting ring analysis, the permeability coefficient of the surrounding rock was fixed at $k_r = 1 \times 10^{-6}$ m/s, and k_r/k_g was set to the same sequence. For both groups, the grouting

ring thickness, primary support thickness, and secondary lining thickness were 3 m, 0.25 m, and 0.30 m, respectively, and the secondary lining permeability coefficient was 1×10^{-10} m/s.

3. Seepage and deformation responses during excavation

3.1. Spatial distributions of seepage and displacement fields

Before excavation, the pore water pressure increased with depth, reaching approximately 2.94 MPa at the tunnel location. After excavation, a low-pore-pressure zone formed around the tunnel periphery, and the pore water pressure gradually recovered from the tunnel wall toward the deeper surrounding rock. In the cross-section, groundwater converged toward the tunnel cavity, with a relatively high seepage velocity near the tunnel wall; in the longitudinal direction, the low-pore-pressure zone advanced with the tunnel face, and water flow concentrated near the tunnel face and the bench interface. The surrounding rock deformation was also mainly distributed around the tunnel periphery and near the tunnel face, decreasing with increasing distance from the excavation boundary.

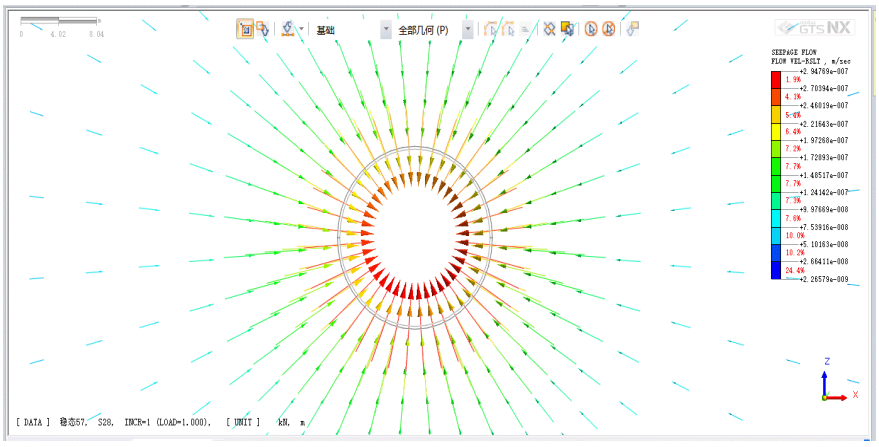

(a) Seepage vectors

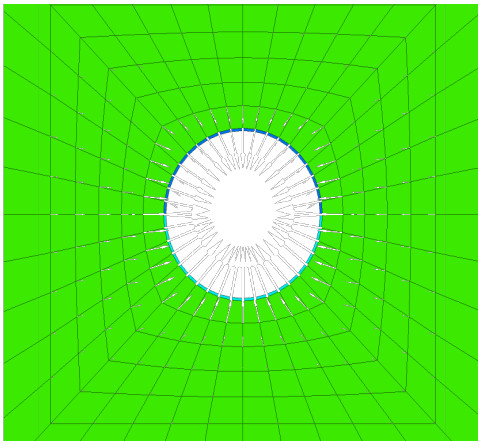

(b) Displacement vectors

Figure 1. Distributions of seepage and displacement in the cross-section after tunnel breakthrough: (a) Seepage Vectors; (b) Displacement Vectors.

Figure 1 indicates that after tunnel breakthrough, groundwater generally enters the tunnel cavity along

the normal direction to the tunnel wall, while the surrounding rock converges inward, with the response relatively concentrated near the invert. During upper bench excavation, the crown and the region near the bench are first disturbed; after lower bench excavation, the response extends to the lower surrounding rock. The longitudinal displacement of the surrounding rock increases as the tunnel face approaches, and face extrusion is pronounced, reflecting the spatial effect of excavation unloading.

3.2. Response of a typical section to construction steps

To analyze the evolution characteristics of seepage and deformation at a typical section during tunnel excavation, a section located 10 m from the tunnel portal was selected. The outflow per unit length and displacement at the crown, haunch, and invert were extracted, and their variation patterns with construction steps were compared. The results are shown in **Figure 2**.

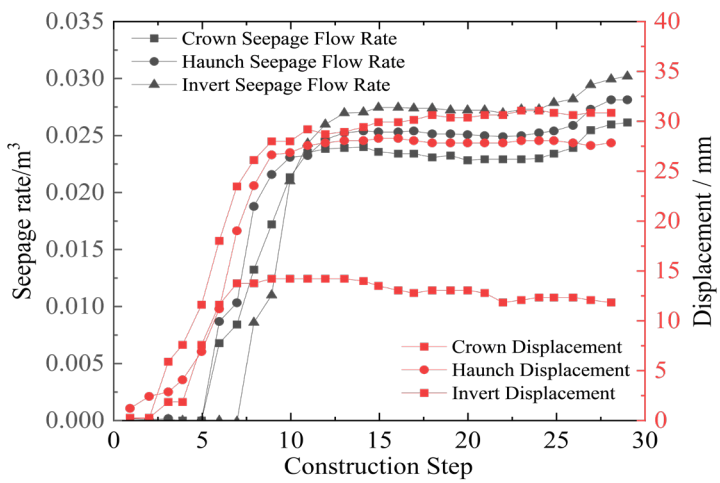

Figure 2. Response of the section 10 m from the tunnel portal to construction steps.

As shown in **Figure 2**, after the studied section is exposed, the outflow at the tunnel wall increases rapidly and then gradually stabilizes with excavation advancement and support installation. The outflow is largest at the invert, followed by the haunch, and smallest at the crown. The surrounding rock displacement begins to develop before the tunnel face reaches the section, accelerates when excavation approaches the studied section, and slows after the tunnel face moves away. The crown exhibits settlement, the haunches converge inward, and the invert experiences heave. Both types of response change markedly near the passage of the excavation through the section, indicating that timely support installation plays an important role in controlling deformation and outflow during this stage.

4. Influence of support thickness on seepage and deformation

4.1. Primary support thickness

As the primary support thickness increases, the displacement amplitudes at all monitoring points gradually decrease, and crown settlement, haunch convergence, and invert heave are all controlled, as shown in **Figure 3**.

When the thickness is relatively small, the displacement change induced by thickening is more pronounced; once the thickness reaches approximately 0.30 m, the curves gradually level off. A thicker primary support enhances the overall stiffness and constraint capacity of the structure around the tunnel, enabling it to effectively share the surrounding rock load and thereby reduce subsequent deformation.

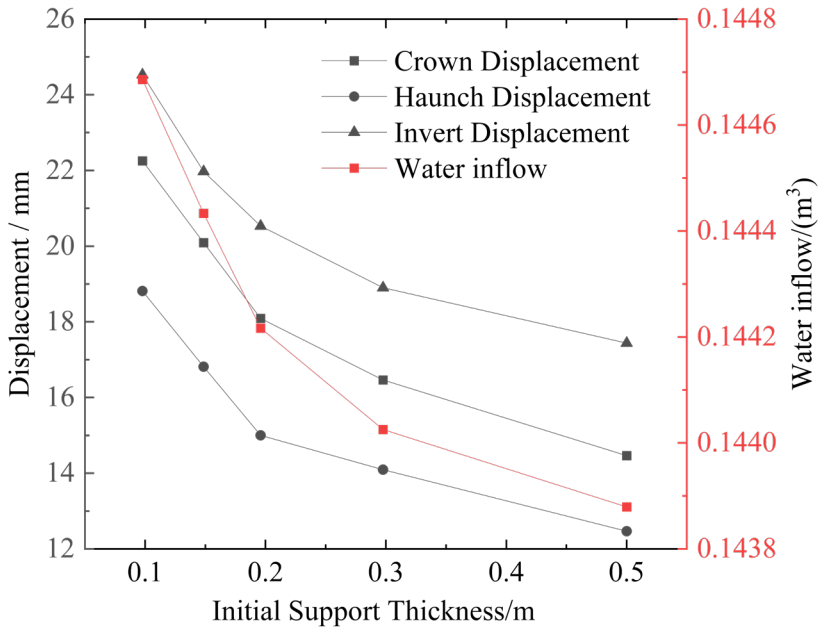

Figure 3. Influence of primary support thickness on the response around the tunnel.

The water inflow around the tunnel decreases with increasing primary support thickness, while the magnitude of this decrease gradually diminishes as shown in **Figure 3**. Thickening the low-permeability primary support lengthens the seepage path through the support layer and increases its hydraulic resistance. Within the calculation range of this group, the variation in water inflow is relatively gentle, indicating that under the given surrounding rock, grouting ring, and lining conditions, the water-control benefit of merely increasing the primary support thickness is limited. Meanwhile, increasing the primary support thickness raises the external water pressure on the lining to some extent, reflecting the redistribution of hydraulic head after the water-blocking effect of the support layer is enhanced.

4.2. Grouting ring thickness

When the grouting ring thickness increases from 1 m to 9 m, the displacement amplitudes around the tunnel decrease overall, as shown in **Figure 4**. At relatively small thicknesses, enlarging the reinforcement zone noticeably improves the confinement around the tunnel; as the thickness continues to increase, the displacement curves gradually level off. Grouting reinforcement enhances the overall bearing capacity of the rock mass within a certain range around the tunnel, allowing the excavation load to be shared by the reinforcement zone and the external surrounding rock.

Water inflow continuously decreases with the thickening of the grouting ring and gradually exhibits a leveling-off trend, as shown in **Figure 4**. Under the same material permeability coefficient, enlarging the grouting zone increases the hydraulic head loss before groundwater reaches the support structure.

Correspondingly, the external water pressure on the lining also decreases as the grouting ring thickness increases. Compared with thickening the primary support, the grouting ring forms a water-blocking zone outside the structure, thereby simultaneously reducing the water inflow into the tunnel and lowering the external water pressure on the lining.

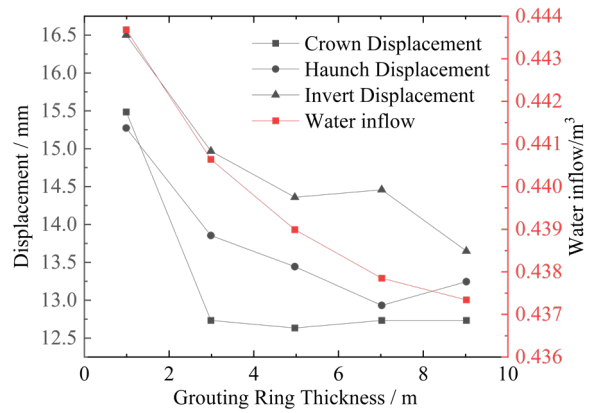

Figure 4. Influence of grouting ring thickness on the response around the tunnel.

5. Influence of material properties on seepage and deformation

5.1. Elastic moduli of primary support and grouting reinforcement zone

As the elastic modulus of the primary support increases, crown settlement, haunch convergence, and invert heave all decrease, and the mechanical response of the lining is correspondingly reduced. When the primary support stiffness is relatively low, increasing the elastic modulus markedly enhances confinement around the tunnel; as the stiffness continues to increase, the reduction in displacement gradually diminishes. A similar trend is observed when the elastic modulus of the grouting reinforcement zone is increased from 1 GPa to 10 GPa, indicating that improving the mechanical properties of the reinforcement zone is beneficial for restricting deformation around the tunnel and reducing the loads borne by subsequent support structures.

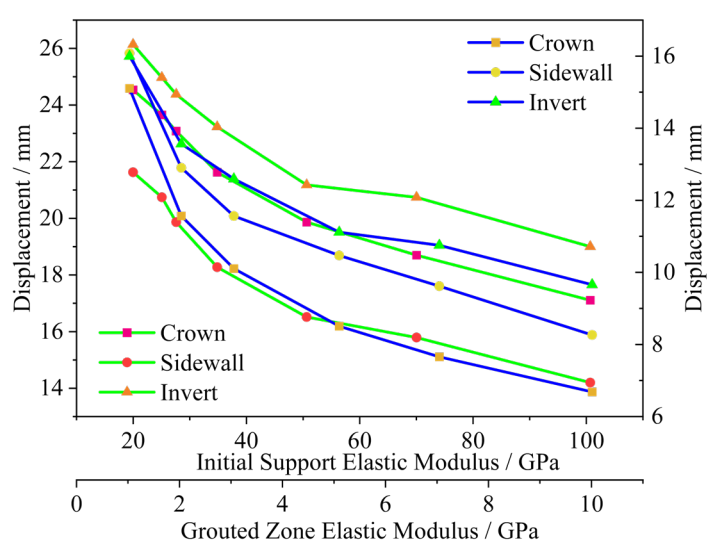

Figure 5. Influence of elastic moduli of the primary support and grouting reinforcement zone on tunnel peripheral displacement.

5.2. Primary support permeability coefficient

With the permeability coefficient of the grouting ring fixed, an increase in k_g/k_l indicates a decrease in the permeability coefficient of the primary support. As shown in **Figure 6**, as this ratio increases from 2 to 200, the water inflow around the tunnel first decreases rapidly and then gradually levels off. At relatively small ratios, changes in the primary support permeability noticeably alter the water inflow into the tunnel; as the ratio increases, the incremental effect of further reducing the primary support permeability coefficient diminishes. The external water pressure on the lining increases with increasing ratio, indicating that enhanced water-blocking by the primary support is accompanied by an increase in water pressure outside the structure.

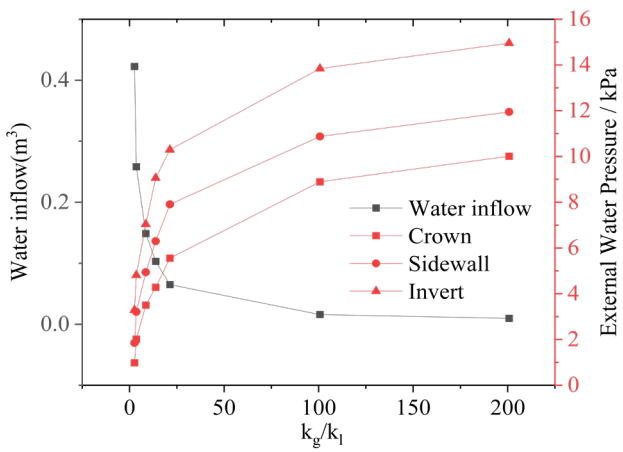

Figure 6. Influence of primary support and grouting ring permeability on water inflow and external water pressure on the lining.

5.3. Grouting ring permeability coefficient

When the permeability coefficient of the surrounding rock is fixed, an increase in k_r/k_g indicates a decrease in the permeability of the grouting ring. As shown in **Figure 7**, the water inflow decreases rapidly with increasing ratio and then transitions to a gradual decline; the external water pressure on the lining decreases synchronously. A low-permeability grouting ring causes more hydraulic head loss to occur outside the support structure, reducing both the amount of water flowing toward the tunnel cavity and the water pressure acting on the outer side of the lining. Both measures have water-control effects; however, the grouting ring can reduce the external water pressure while decreasing water inflow, and its effect is clearly different from that of the primary support.

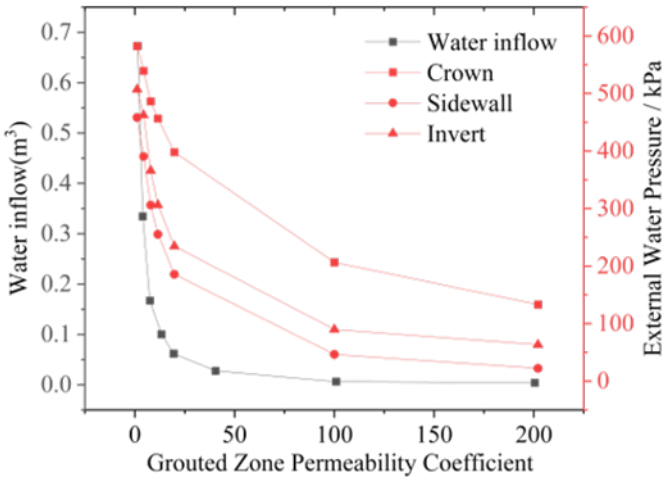

Figure 7. Influence of primary support and grouting ring permeability on water inflow and external water pressure on the lining.

6. Conclusions

(1) After bench excavation, groundwater converges toward the tunnel cavity and tunnel face, while the surrounding rock deforms toward the excavated space, with more pronounced responses concentrated around the tunnel periphery and near the tunnel face. The responses change markedly as the tunnel face approaches and passes the studied section, and then gradually stabilize with support installation and as the excavation face moves away.

(2) Increasing the thickness of the primary support and grouting ring can reduce the peripheral displacement and water inflow, and the incremental control effect gradually diminishes as the thickness increases. Increasing the elastic modulus of the primary support and grouting reinforcement zone can further restrict the deformation of the surrounding rock, and this effect also tends to level off gradually.

(3) Reducing the permeability coefficients of both the primary support and the grouting ring can decrease tunnel water inflow. When the water-blocking capacity of the primary support is enhanced, the external water pressure on the lining increases, whereas when the water-blocking capacity of the grouting ring is enhanced, the external water pressure decreases. The selection of support and grouting parameters should comprehensively account for deformation control, water inflow control, and structural water pressure.

Disclosure statement

The author declares no conflict of interest.

References

[1] Liu H, Liu J, Zhang Y, et al., 2020, Experimental Study on the Mechanical Properties of Fractured Limestone Under Unloading Confining Pressure Damage. Water Power, 46(3): 28–32 + 60.

[2] Li K, Yang B, Qin Q, 2019, Experimental Study on Unloading Damage and Permeability of Dolomite Based on Nuclear Magnetic Resonance Technique. Chinese Journal of Rock Mechanics and Engineering, 38(S2):

3493–3502.

[3] Wang R, Xu B, Xu W, et al., 2019, Experimental Research of the Influence of Different Unloading Stress Paths on Permeability Evolution of Sandstone. Chinese Journal of Rock Mechanics and Engineering, 38(3): 467–475.

[4] Wang R, Li J, Jiang Y, et al., 2010, Experimental Study of Influence of Excavation Unloading on Mechanical Properties of Sandstone. Rock and Soil Mechanics, 31(S1): 156–162 + 206.

[5] Li H, Xia C, Yan Z, et al., 2007, Study on Marble Unloading Mechanical Properties of Jinping Hydropower Station Under High Geostress Conditions. Chinese Journal of Rock Mechanics and Engineering, 26(10): 2104–2109.

[6] Liu X, Lin Y, Kong J, 2007, Study of Hydro-Mechanical Coupling of Fractured Rock Masses Considering Unloading Effect. Rock and Soil Mechanics, 28(S1): 192–196.

[7] Liang N, Liu X, Ai W, et al., 2011, Experiment Study on the Permeability of Fractured Rock Under Unloading. China Civil Engineering Journal, 44(1): 88–92.

[8] Code for Design of Railway Tunnel: TB 10003—2016, 2016, Beijing: China Railway Publishing House.

[9] Liu Z, 2015, Study on Mechanism and Control Technology of Interaction Between Fractured Rock Mass Tunnel and Groundwater Environment, thesis, Beijing Jiaotong University.

[10] Zhang H, 2014, Seepage Analysis of Groundwater and Study on Treatment Measures of Pouring Water in WuDuxi Highway Tunnel, thesis, Chang'an University.

Publisher's note

Bio-Byword Scientific Publishing remains neutral with regard to jurisdictional claims in published maps and institutional affiliations.